

A Planar Picoamperemeter Based on a Superconducting Quantum Interferometer

E. V. Burmistrov, P. N. Dmitriev, M. A. Tarasov, A. S. Kalabukhov, S. A. Kovtonyuk,
S. A. Gudoshnikov, O. V. Snigirev, L. S. Kuz'min, and V. P. Koshelets

Received September 8, 2005

Abstract—An optimized picoamperemeter based on a superconducting quantum interferometer device (SQUID) for a metal cold-electron bolometer is fabricated and experimentally studied. The intrinsic SQUID current noise caused by the input coil is estimated to be less than $1 \text{ pA/Hz}^{1/2}$. Owing to the application of modulation electronics, current sensitivity in the input coil reaches $5 \text{ pA/Hz}^{1/2}$ in the frequency band from 10 Hz to 10 kHz.

PACS numbers: 85.25.Dq, 85.25.-j

DOI: 10.1134/S1064226906110143

INTRODUCTION

Readout is still one of the main challenges in the design of bolometers and direct detectors, which are sensitive over the range from millimeters to X-rays. Consider, for example, a normal metal hot-electron bolometer (NHEB) with superconductor/insulator/normal metal (SIN) tunnel junctions [1]. Of particular interest is the operation of such a bolometer in the voltage bias mode, in which case, the data should be read by an amperemeter. A SQUID-based femtoamperemeter for NHEB readout was fabricated and tested in [2]. The amperemeter had an additional cryogenic transformer and showed the best sensitivity, $35 \text{ fA/Hz}^{1/2}$, at 1 kHz. The input impedance of the system was $6 \text{ k}\Omega$ at 1 kHz, which agrees with the 0.9-H inductance of the input coil of the transformer. Note that, for signal sources with a resistance below $1 \text{ k}\Omega$, the input inductance should be reduced; otherwise, the amperemeter will act as a voltmeter. Another difficulty is that the flicker noise produced by a cryogenic transformer with a ferromagnetic core increases greatly at frequencies below 1 kHz, while the frequency range of highly sensitive bolometers extends to several hertz or lower. (The lowest frequencies are of the most interest and most difficult to detect.) Therefore, matching the SQUID amperemeter to a bolometer with a resistance of about $1 \text{ k}\Omega$ is still a problem.

A new concept of a cold-electron bolometer [3] also involves a sensitive SQUID-based readout device. Such a bolometer could find use, for example, in the currently developed OLIMPO balloon project [4], where the required sensitivity of detectors is about $1.2 \times 10^{-17} \text{ W/Hz}^{1/2}$. Hence, the current sensitivity of a readout unit should be about $1 \text{ pA/Hz}^{1/2}$ (depending on the signal frequency and the background load) and reach $0.1 \text{ pA/Hz}^{1/2}$ for low-frequency channels.

The aim of this study is to further investigate a SQUID-based current meter. Technically, the task was divided into the following parts: fabrication of SQUIDs with planar input transformers by means of the production technology of niobium superconductor/insulator/superconductor (SIS) junctions and attainment of the current-sensitivity level of $1 \text{ pA/Hz}^{1/2}$ for a single SQUID.

1. THE SQUID FABRICATION TECHNOLOGY

The results presented in [2] were obtained for the SQUIDs fabricated by VTT (Finland) [5, 6]. Serial VTT SQUIDs could not be used readily in this study since they have a low normal resistance. With a number of design modifications, special-purpose SQUIDs were fabricated and tested. Figure 1 shows a schematic diagram and microphotograph of the fabricated sample.

The SQUID amperemeter is a superconducting quantum interferometer integrated with an input coil on a single chip. The employed fabrication method consists of seven stages.

(i) Formation of a base electrode. A photoresist mask specifying the geometry of the base electrode is formed on a silicon substrate with a 100-nm-thick Al_2O_3 layer preliminarily evaporated to protect the substrate material during the junction formation by plasma-chemical etching. Then, a three-layer Nb–Al/AIO_x–Nb structure is deposited by the magnetron sputtering method. The layers have thicknesses of 180, 7, and 80 nm, respectively. All layers are evaporated in a single vacuum cycle. The evaporated aluminum is oxidized in pure oxygen to form a tunnel barrier. The critical current density of SIS junctions depends on the oxygen pressure and the oxidation time. The base

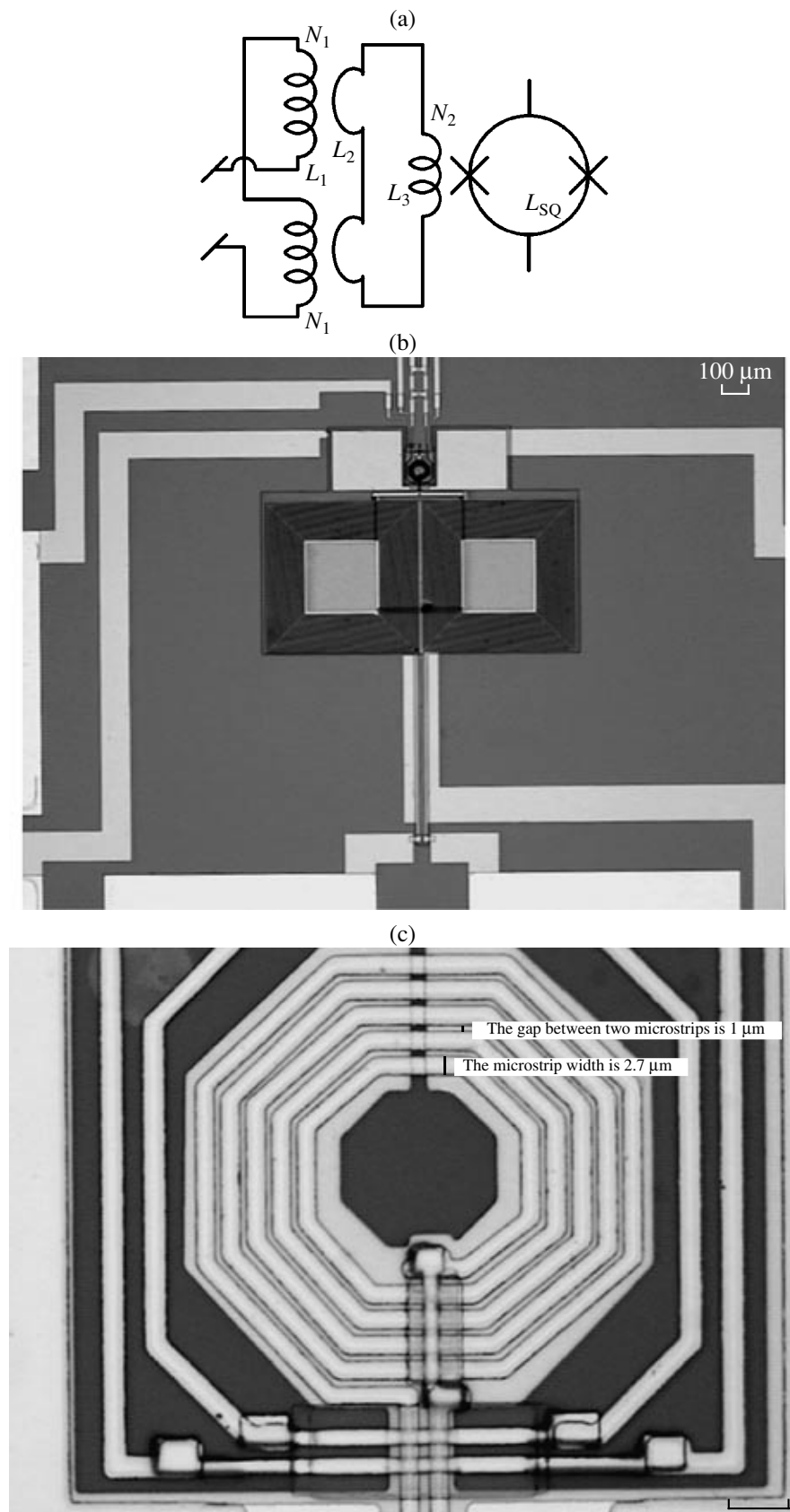


Fig. 1. (a) Schematic diagram and (b) microphotograph of the planar SQUID fabricated integrally on a chip; (c) microphotograph of the central part of the SQUID.

electrode is formed by the lift-off method in an ultrasonic bath of acetone or another solvent.

(ii) Formation of SIS junctions by the plasma-chemical etching in CF_4 plasmas. The three-layer structure is covered by a photoresist mask of the junction pattern, and the upper Nb layer is removed. After the etching, a 300-nm-thick SiO_2 layer ($\epsilon = 4.0 \pm 0.4$) is evaporated through the same mask. The contacts to the junctions are opened in acetone by the lift-off method. In order to reproduce junction sizes better, the photoresist is exposed to light twice and each of the SQUID junctions is formed at the intersection of two strips superimposed crosswise.

(iii) Formation of shunts. The shunts are formed by evaporating a resistive Mo layer with a surface resistance of 2Ω per square through the photoresist mask by the subsequent lift-off process.

(iv) Formation of the upper electrode. A 300-nm-thick Nb layer is evaporated through the photoresist mask by the subsequent lift-off process.

(v) Formation of the insulator for the contacts of the coils. A 450-nm-thick SiO_2 layer is evaporated through the photoresist mask by the subsequent lift-off process.

(vi) Formation of the contacts of the coils. A 400-nm-thick Nb layer is evaporated through the photoresist mask by the subsequent lift-off process.

(vii) Evaporation of gold contact pads through the photoresist mask by the subsequent lift-off process.

The SQUID was designed as an octagonal loop (the inner dimension is $24 \mu\text{m}$) formed by 5 turns of the input coil and a gradiometric transformer with two $230\text{-}\mu\text{m}$ square openings and 22 turns of the input coil in each half. The size of the Josephson junctions is $2 \times 2 \mu\text{m}^2$. The calculated parameters of the SQUID are as follows: the normal resistance R_N is 3Ω ; the inductance of the input coil, L_1 , is 250 nH ; the inductance of the transformer loop, L_2 , is 250 pH ; the inductance of the small input coil, L_3 , is 750 pH ; the number of turns of the primary transformer, N_1 , is 22; the number of turns of the secondary transformer, N_2 , is 5; and the inductance of the interferometer loop, L_{SQ} , is 30 pH .

The fabricated SQUIDS exhibited a good reproducibility of parameters, and the maximal critical current reached $15 \mu\text{A}$. Figure 2 shows the most important working characteristic of a SQUID: output voltage V versus current in input coil I_{in} . The maximum peak-to-peak voltage swing is $42 \mu\text{V}$. With the use of the simple approximation $V_{pp}/|V_\Phi| = \Phi_0/\pi$ (Φ_0 is a unit of one flux quantum equal to $2.07 \times 10^{-15} \text{ Wb}$) [7], it is possible to obtain from the curve that $dV/d\Phi = 132 \mu\text{V}/\Phi_0$. A highly precise value of current sensitivity in the input

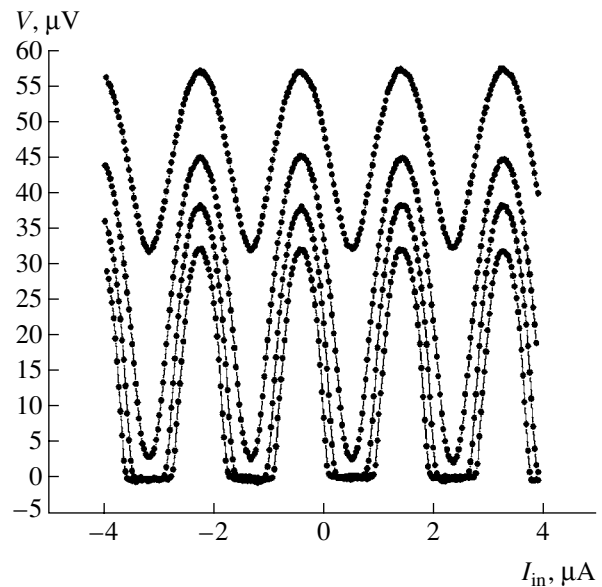


Fig. 2. Flux-voltage characteristic of the SQUID.

coil was measured with electronics in the flux-trapping mode, thereby yielding $dI_{\text{in}}/d\Phi = 1.25 \mu\text{A}/\Phi_0$.

2. MEASURING CURRENT SENSITIVITY OF THE PLANAR SQUID

First of all, it is necessary to determine the sensitivity of the system without an additional transformer at the input. The measurements were performed in the flux-loaded loop (FLL) mode on the circuit shown in Fig. 3. In contrast to [2], the low-frequency noise was reduced by using modulation electronics with a 4-MHz modulation frequency. The advantages and disadvantages of such circuits utilizing a SQUID as a null detector are described in detail in [7]. The electronics' noise at the amplifier input was $1 \text{ nV}/\text{Hz}^{1/2}$. A matching cold transformer with a transformation ratio of 10 was connected between the SQUID and the amplifier. During the measurements, the SQUID chip and the cold transformer were held at 4.2 K .

The equivalent noise current caused by the input coil is the main characteristic of a SQUID current meter and is determined from the equivalent value of flux noise in the SQUID circuit. This characteristic was measured by an HP35665A low-frequency spectrum analyzer in the FLL mode. The SQUID electronics were tuned to the value $dV/d\Phi = 5 \text{ V}/\Phi_0$, which corresponded to the optimum operation of the electronics itself. The noise-voltage spectral density measured at the output of the SQUID electronics was $S_V^{1/2} = 20 \mu\text{V}/\text{Hz}^{1/2}$. The flux noise in the interferometer ring is taken as the product of the noise voltage density and the slope of the volt-

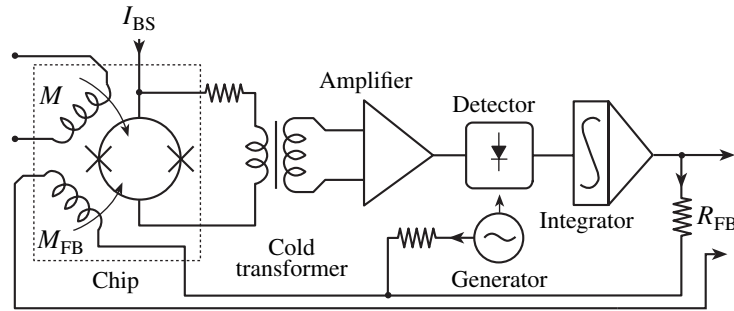


Fig. 3. Schematic diagram of a SQUID circuit with modulation electronics. A cold transformer is used to match the SQUID to the amplifier.

age-flux characteristic: $S_{\Phi}^{1/2} = S_V^{1/2} dV/d\Phi = 4 \mu\Phi_0/\text{Hz}^{1/2}$.

With the use of this value and the current-to-flux conversion factor measured previously, it is possible to obtain the total equivalent noise current of the SQUID amperemeter, including the noise of the electronics and other interferences: $S_I^{1/2} = S_{\Phi}^{1/2} dI/d\Phi = 5 \text{ pA}/\text{Hz}^{1/2}$. It is seen from Fig. 4 that the circuit without the additional transformer covers the entire required frequency range: from several kilohertz to several hertz.

The known formula (see [8]) for the noise flows in the interferometer ring

$$S_{\Phi} = 18 \frac{k_B T L^2}{R},$$

yields a value of $0.6 \mu\Phi_0$, which is smaller than the experimental result, $4 \mu\Phi_0$. This underestimation is due to the fact that the resulting sensitivity depends not only on the SQUID but also on the properties of the whole system. In measurements without the additional transformer, a possible method of approaching the calculated value is to improve the matching between the SQUID and the electronics via the cold transformer and to reduce the noise in all electronic components. In this case, the current sensitivity is limited to $0.7 \text{ pA}/\text{Hz}^{1/2}$.

3. SENSITIVITY OF THE PICOAMPEREMETER WITH THE ADDITIONAL TRANSFORMER

As mentioned above, the sensitivity of the SQUID amperemeter is determined by (i) characteristics of the SQUID integrated on a single chip with the input coil and (ii) the degree of matching of the amperemeter to a detector by means of the additional transformer. A schematic diagram of the SQUID amperemeter with the

additional transformer is shown in Fig. 5. This system can be described by the following system of equations:

$$\begin{cases} M_T^2 = k_T^2 L_{T1} L_{T2} \\ i\omega I M_T + i\omega I_2 M_1 = i\omega I_1 (L_{T2} + L_1) \\ i\omega I_1 M_1 + i\omega I_{SQ} M_2 = i\omega I_2 (L_2 + L_3) \\ i\omega I_2 M_2 = I_{SQ} \left(\frac{1}{i\omega\Lambda} + \frac{1}{\Theta} \right)^{-1}, \end{cases} \quad (1)$$

where the interferometer is represented by a parallel connection of dynamic resistance Θ and inductance Λ . In [9] by Clarke and Hilbert, the dependencies of Θ and Λ on the magnetic flux in the interferometer are measured and studied in detail. The values of the parameters of our interferometers are close to those of the interferometers considered in [8]. Therefore, it is possible to use the estimates $R_N/20$ and $5L_{SQ}$ obtained in [8] for the values of Θ and Λ at the optimal working point.

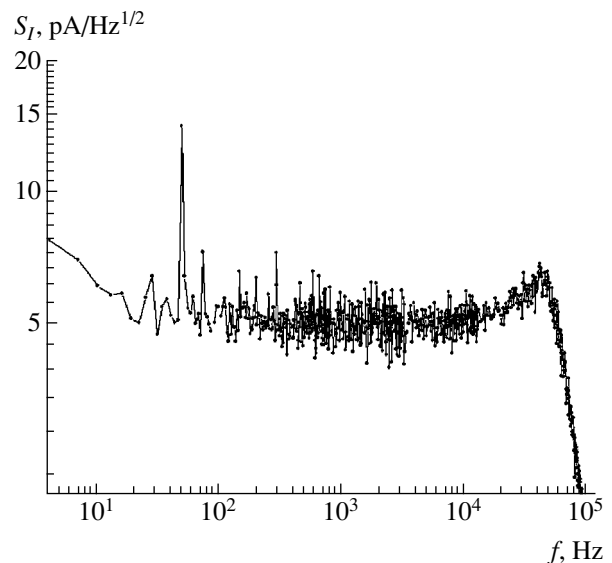


Fig. 4. Total system noise converted to the SQUID input.

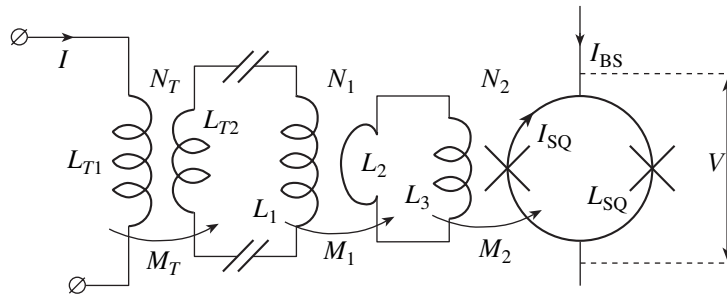


Fig. 5. Schematic diagram of the SQUID with the additional transformer.

Transformer L_1, L_2 is necessary to increase the current sensitivity at the input of coil L_1 . For simplicity sake, circuit L_2, L_3 can be eliminated; as a result, inductances L_1 and L_2 and mutual inductances M_1 and M_2 are replaced by equivalent mutual inductance M (Fig. 6). Then, the system can be rewritten as

$$\begin{cases} IM_T + I_{SQ}M = I_1(L_{T2} + L_X) \\ i\omega I_1 M = I_{SQ} \left(\frac{1}{i\omega\Lambda} + \frac{1}{\Theta} \right)^{-1}; \end{cases} \quad (2)$$

$$M = \frac{M_1 M_2}{L_2 + L_3}, \quad (3)$$

$$L_X = L_1 \left(1 - k_1^2 \frac{L_2}{L_2 + L_3} \right), \quad (4)$$

$$L_Y = L_{SQ} \left(1 - k_2^2 \frac{L_3}{L_2 + L_3} \right), \quad (5)$$

where $k_1^2 = M_1^2/L_1L_2$ and $k_2^2 = M_2^2/L_3L_{SQ}$.

The noise flux in the interferometer, $\delta\Phi$, determines the noise current $\delta I_1 = \frac{\delta\Phi}{M}$. Thus, it is possible to obtain a formula for the noise in the input turn of the additional transformer, i.e., the resolution limit due to the SQUID noise:

$$\delta I = \frac{\sqrt{(\delta\Phi)^2 \left[\left(L_{T2} + L_X - \frac{M^2}{\Lambda} \right)^2 + \omega^2 \frac{M^4}{\Theta^2} \right]}}{\sqrt{M_T^2 M^2}}. \quad (6)$$

This expression is convenient for estimating the sensitivity of the amperemeter because it contains equivalent mutual inductance M , which can be obtained from the voltage-flux characteristic of the SQUID (see Fig. 2) as the reciprocal of $dI/d\Phi$.

Since $L_{T2} \gg L_X - \frac{M^2}{\Lambda}$ and $(L_{T2})^2 \gg \omega^2 \frac{M^4}{\Theta^2}$, for rough estimation, formula (6) can be reduced to the form

$$\delta I \approx \frac{\delta\Phi}{M_T M} L_{T2}. \quad (7)$$

However, this simplification is admissible only for frequencies below 100 kHz [2], since at higher values, the equivalent impedance of the SQUID significantly increases and the system begins to operate as a voltmeter.

In terms of the intrinsic inductances of the coils included in the system (see Fig. 5), formula (7) appears as

$$\delta I = \frac{\delta\Phi}{k_1 k_2 k_T} \frac{\sqrt{(L_2 + L_3)^2 L_{T2}}}{\sqrt{L_{T1} L_1 L_2 L_3 L_{SQ}}}. \quad (8)$$

It can be seen easily from (8) that an increase in the input inductance of the additional transformer (L_{T1}) will raise the current sensitivity of the SQUID system. However, there are two factors that limit this inductance. First, the system must always remain an amperemeter; i.e., its input impedance must remain much lower than the resistance of the bolometer. For example, operation at a frequency of 1 kHz requires that the input inductance be smaller than 100 mH. In this case, the maximal

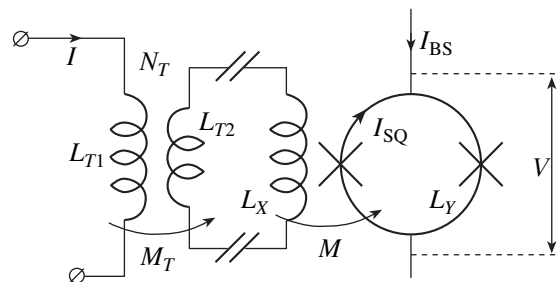


Fig. 6. Schematic diagram of the SQUID with the additional transformer. Circuits L_2 and L_3 are excluded.

transformation ratio approaches $n = \sqrt{L_{T1}/L_1} = 500$ (on the condition that $L_{T2} = L_1$). This means that the 5-pA/Hz^{1/2} sensitivity provided in the system without an additional transformer will be improved to 10 fA/Hz^{1/2} with the additional transformer.

One more important limitation on the input inductance of the additional transformer is associated with the transmission bandwidth of the SQUID readout, Δf , which is related to the energy resolution of the bolometer:

$$\varepsilon = \text{NEP}/\sqrt{\Delta f}, \quad (9)$$

where NEP is the noise equivalent power of the bolometer. Since $\Delta f = R_b/2\pi L_{T1}$, the energy sensitivity of the bolometer deteriorates with an increase in the transformation ratio (i.e., in the input sensitivity):

$$\varepsilon = n(\text{NEP}) \sqrt{\frac{2\pi L_1}{R_b}}. \quad (10)$$

Thus, the design of an optimal additional transformer should be a trade-off. The most promising variants are a superconducting planar transformer with a comparatively large (10 mm) inner dimension of the loop and an air transformer with a superconducting secondary winding.

CONCLUSIONS

A planar integrated SQUID picoamperemeter intended for readout of data from a cold-electron bolometer has been designed, fabricated, and optimized. The intrinsic SQUID noise converted into the equivalent current noise in the input coil has been found to be within 1 pA/Hz^{1/2}. The use of modulation electronics allowed us to significantly reduce the 1/f noise in the system and achieve a 5-pA/Hz^{1/2} current sensitivity in the input coil in the frequency range from 10 Hz

to 10 kHz. The performance of the additional transformer has been analyzed and optimized for coupling the SQUID amperemeter to a bolometer. It has been estimated that the proposed SQUID circuit coupled to a bolometer with a resistance of 1 k Ω will operate as a femtoamperemeter with a limiting resolution of 10 pA/Hz^{1/2} at 1 kHz.

ACKNOWLEDGMENTS

This study was supported by the Federal Agency for Science and Innovations (state contract nos. 02.434.11.10.10 and 02.434.11.70.31), President of the Russian Federation Grant Council (grant no. NSh 7812.2006.2), and the International Science and Technology Center (grant no. 3174).

REFERENCES

1. L. Kuzmin and D. Golubev, *Physica C* **372–376**, 378 (2002).
2. M. Tarasov, A. Kalabukhov, S. Kovtonyuk, et al., *Radiotekh. Elektron. (Moscow)* **48**, 1521 (2003) [*J. Commun. Technol. Electron.* **48**, 1404 (2003)].
3. L. Kuzmin, in *Millimeters and Submillimeters Detectors (Proc. SPIE Conf., Glasgow, UK, June 21–25, 2004)* (Bellingham, Wash.: SPIE, 2004), Vol. 5498, pp. 349–361.
4. S. Masi, P. Ade, A. Boscaleri, et al., in *Proc. 16th ESA Symposium on European Rocket and Balloon Programmes and Related Research, St. Gallen, Switzerland, June 2–5, 2003* (ESA, St. Gallen, 2003), No. ESA-SP-530, p. 557.
5. H. Seppa, M. Kiviranta, A. Satrapinski, et al., *IEEE Trans. Appl. Supercond.* **3**, 1816 (1993).
6. M. Kiviranta and H. Seppa, *IEEE Trans. Appl. Supercond.* **5**, 2146 (1995).
7. D. Drung, *Supercond. Sci. Technol.* **16**, 1320 (2003).
8. C. Tesche and J. Clarke, *J. Low Temp. Phys.* **29** (3–4), 301 (1977).
9. H. Hilbert and J. Clarke, *J. Low Temp. Phys.* **61** (3–4), 237 (1985).